available at www.sciencedirect.com

ScienceDirect

journal homepage: www.ejconline.com

Ethidium bromide as a vital probe of mitochondrial DNA in carcinoma cells

*Anna Maria Villa, Silvia Maria Doglia**

Department of Biotechnology and Biosciences, University of Milano-Bicocca, Piazza della Scienza 2, 20126 Milan, Italy
Consorzio Nazionale Interuniversitario per le Scienze fisiche della Materia (CNISM) UdR Milano-Bicocca, via Cozzi 53, 20125 Milan, Italy

ARTICLE INFO

Article history:
Received 27 March 2009
Received in revised form 17 June 2009
Accepted 24 June 2009
Available online 27 July 2009

Keywords:
Ethidium bromide
Human carcinoma cells
Laser scanning confocal fluorescence microscopy
Mitochondria
mtDNA
Mitochondria morphology
Mitochondria populations
Multidrug resistance
Rhodamine 123

ABSTRACT

The interaction of ethidium bromide (EB) with mitochondria in human breast and lung carcinoma cells was investigated under living conditions, employing a laser scanning confocal fluorescence microscopy (LSCFM) with a photon counting detection to reduce drastically the laser power excitation and the fluorescent probe concentration. In sensitive and multidrug resistant MCF-7 cell lines, which are important model systems for the study of mitochondria in tumour cells, two distinct populations of mitochondria were observed, each characterized by a different EB fluorescence, membrane potential, cellular localization and morphology. By image analysis, these peripheral mitochondria showed a peculiar morphology, consisting of punctuate organelles (0.8 μm in size) organized in rosette-like assemblies. Unexpectedly, an intense EB fluorescence was observed in these mitochondria, indicating a high accessibility to EB of their mtDNA, which is likely to be in an active replicative or transcriptional state. These results might, therefore, suggest an active biogenesis and metabolism of the peripheral mitochondria that could be a consequence of the increased energetic needs of the cells, after their tumour transformation. Indeed, the pool of peripheral mitochondria, as well as their peculiar morphology and spatial organization, were found to be a characteristic feature of all the carcinoma cells examined here, but not of their non-transformed parental MCF10A cells.

1. Introduction

Mitochondria not only play a central role in cell physiology and metabolism, but are also involved in the regulation of cell proliferation, differentiation and apoptosis, as widely shown by several studies over the last decades.[1] The impairments of these processes have been found to be the hallmark of neurodegenerative diseases[2] and cancer.[3] Indeed, altered mitochondria regulation of apoptosis[1] and cell metabolism[4,5] – in addition to mtDNA mutations,[6] were observed in several types of cancer cells. Whether these dysfunctions are among the causes or if they are secondary effects of the tumour transformation is still an open question.

Surprisingly, mtDNA seems to be involved in different ways in the tumour transformation. In particular, in prostate cancer cells the mtDNA depletion has been recently found to activate the hypermethylation of nuclear DNA promoters,[7] an epigenetic alteration that is involved in the early development of cancer.[8] Moreover, an overexpression of proteins coded by mtDNA, due to an enhanced transcription of the mitochondrial genome, was reported to occur after the malignant transformation of human dermal fibroblasts and in lymphomas.[9,10]

All these results suggest that mitochondria and mtDNA play a crucial role in the onset and progression of cancer. However, in spite of a large number of studies, mitochondria

* *Corresponding author:* Tel.: +39 02 6448 3459; fax: +39 02 6448 3565.
E-mail address: silviamaria.doglia@unimib.it (S.M. Doglia).
0959-8049/$ - see front matter © 2009 Elsevier Ltd. All rights reserved.
doi:10.1016/j.ejca.2009.06.022

regulation of cell metabolism and mtDNA activity in tumour cells are not yet fully understood. To address these issues, non-invasive fluorescence imaging microscopies could be very promising, since in recent years these techniques were proved to be successful tools for the study of mitochondria in single living cells.[11–15] In particular, mtDNA has been studied in living cells by fluorescence microscopy using ethidium bromide (EB), a DNA intercalating fluorescent probe known to stain nucleic acids in living cells,[16–18] and whose fluorescence has been found to vary with the conformational status of DNA.[12,17–19] EB is well known to enter living cells and to stain mitochondria, but it is not a potentiometric probe, as demonstrated in Refs. [16] and [24]. Instead, its ability to accumulate in mitochondria is due to its high affinity for RNA and DNA. In the last years EB has been used in living cells as a probe of mtDNA to study mtDNA structural changes,[12,19] to demonstrate the presence of mtDNA nucleoids in mitochondria of human cells,[20] and to monitor the dynamics of nucleoids.[21]

In a previous work,[22] we reported a laser scanning confocal fluorescence microscopy (LSCFM) study of mitochondria in carcinoma cells. Working at low power excitation and using sensitive photon counting detection, it has been possible to detect mitochondria under living conditions at high spatial resolution after the staining with rhodamine 123 (R123), a well-known potentiometric probe of mitochondria.[23] Unexpectedly, two independent mitochondria populations were observed in breast carcinoma MCF-7 cells and in lung carcinoma A549 cells. These two populations were found to be different in intracellular localization, morphology and membrane potential.

Considering the crucial role played by mtDNA in cancer transformation, we examined the interaction of mitochondria with EB by LSCFM, to explore the status of mtDNA in the mitochondria populations of carcinoma cells under living conditions.

We report here the results of this study in the carcinoma cell lines previously investigated,[22] including the human breast carcinoma MCF-7 cell lines that are a good model system for the study of mitochondria in tumour cells[23,24]. In all the examined carcinoma cell lines, the two pools of mitochondria were characterized by a distinct EB fluorescence intensity, indicating a different interaction of the dye with mtDNA. These results also demonstrate that EB cannot be taken as an overall marker of mtDNA.

2. Materials and methods

2.1. Chemicals

Rhodamine 123 (R123), ethidium bromide (EB) and verapamil were purchased from Molecular Probes (Eugene, OR). The concentration of the stock solutions of R123 and EB were determined spectrophotometrically.

2.2. Cell cultures

The human breast carcinoma MCF-7 cells and its multidrug resistant (MDR) subline MCF-7/DX overexpressing the Pgp-170 glycoprotein were a kind gift of Prof. M. Manfait (Reims University, Reims, France). The data obtained on these cells were confirmed repeating the experiments on sensitive and MDR MCF-7 cell lines from Dr. G. Arancia (Istituto Superiore di Sanità, Roma, Italy), who also provided the human lung carcinoma A549 cell line. A549 cells were resistant to doxorubicin and overexpressed the lung resistance-related protein (LRP).

MCF-7, its resistant subline and A549 cells were grown in RPMI 1640 (Hyclone, Cramlington, UK) supplemented with 10% v/v FCS (Hyclone), 2 mM L-glutamine, 100 U/ml penicillin and 100 μg/ml steptomycin at 37 °C, 5% v/v CO_2.

The immortalized epithelial MCF-10A cells were grown in DMEM medium (Gibco, Invitrogen) supplemented with 10% v/v FCS, 10 μg/ml insulin, 0.5 μg/ml hydrocortisol and 20 ng/ml EGF at 37 °C, 5% v/v CO_2 in a humidified atmosphere.

2.3. Sample preparation

Cells were seeded in 35 mm Petri dishes and left to grow up to 50–70% confluence. Then the medium was removed, the cells were washed twice with phosphate buffer saline (PBS) and incubated in the growth medium at 37 °C, 5% v/v CO_2 in the presence of the appropriate dye or drug. After incubation, the cells were again washed twice with PBS. Few microliters of PBS were left in the Petri dish to avoid cell drying, and a coverslip was placed over the cells.

For R123 staining, the cells were incubated in a solution of 1 μM R123 for 10 minutes, and, for EB staining, in a 1 μM EB solution for 30 min. For the double staining experiment the cells were incubated with 1 μM EB for 30 min. After 20 min a small volume of R123 stock solution was added to reach the final concentration of 1 μM in the Petri dish.

For the experiment with verapamil, cells were preincubated for 10 min at 37 °C, 5% v/v CO_2 with 100 μM verapamil. Then a small volume of a solution of R123 or EB was added to reach the final concentration of 1 μM. Incubation times were the same as for the staining without verapamil.

2.4. Confocal fluorescence microscopy with photon counting detection

Mitochondria fluorescence in living cells was studied by laser scanning confocal microscopy using the Bio-Rad MRC-600 microscope (Bio-Rad, Hemel Hempstead, UK) coupled with an upright epifluorescence microscope Nikon Optiphot-2 (Nikon, Tokyo, Japan) and equipped with a 60× Nikon Planapochromat oil immersion objective (N.A. = 1.4). Fluorescence was excited at 488 nm using a 25 mW argon laser and the emission was detected above 515 nm. The high sensitivity of photon counting detection was exploited to minimize laser excitation power (0.1 mW at the entry of the optical head) and preserve cell viability and functions.[22] At this excitation power a fluorescent signal of less then 10 photon per pixel – typically of about 3 photons – was detected employing the fast photon counting of the MRC 600 confocal microscope, well below the linearity limit of the detection system. The accumulation of 50–100 frames enable to collect images with a reduced noise level, even from low fluorescent signals. The linearity of this detection allows to quantitatively evaluate

and compare the fluorescence intensity of different images acquired under the same conditions.

Image analysis was performed using the LaserPix software (Bio-Rad). The morphological filter *black top hat* was used to detect mitochondria shape and organisation.

3. Results

3.1. *Mitochondria in carcinoma MCF-7 cells*

The LSCFM images of sensitive human breast carcinoma MCF-7 cells after EB staining (Fig. 1A) allowed us to identify two pools of mitochondria in this cell line: mitochondria with high EB fluorescence at the cell periphery, in the subplasmalemma region, and mitochondria with very weak fluorescence in the central cytoplasm. This result is different from what is observed for the same cells after R123 staining (Fig 1B), where only central mitochondria were seen to be highly fluorescent.[22] Since R123 is a potentiometric probe,[23] the two pools of mitochondria were, therefore, differing in their energetic state, with central mitochondria having a high membrane potential, but not the peripheral ones. We should also note that nucleoli are stained by EB, as can be seen in Fig. 1A and E.

The spatial relationship between these two pools of mitochondria within MCF-7 cells can be better appreciated in Fig. 1E–G, where the double staining experiment with EB and R123 is reported. The merged image of Fig. 1G shows the mitochondria stained with R123 (in green) spreading in cytoplasm from the perinuclear region, while mitochondria stained by EB (in red) are confined to the cell periphery. These mitochondria show a punctate morphology and an unusual organization that can be better appreciated after image analysis. To fully exploit the resolution and contrast capacity, the image analysis has been performed on the data from EB and R123 single staining experiments of Fig. 1A and B. In order to highlight the mitochondria profile, the morphological *black top hat* filter has been applied. As can be seen in Fig. 1C and D, peripheral mitochondria are small round organelles - of about 0.8 micron in size (SD = 0.1 μm) – organized in rosette-like clusters, each formed by few organelles (about 5).

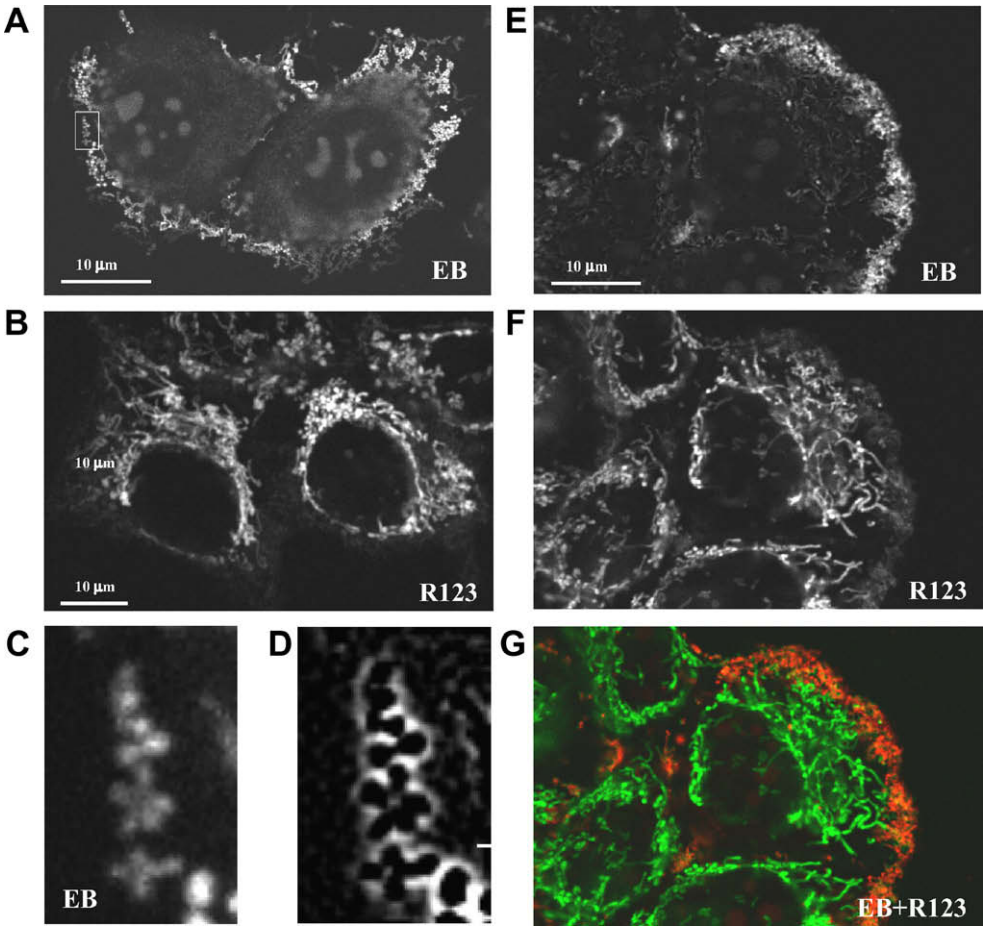

Fig. 1 – Fluorescence images of mitochondria in human breast MCF-7 carcinoma cells. Peripheral mitochondria can be seen in (A) after EB staining, while central mitochondria are observed in (B) after R123 staining; (C) enlarged image of peripheral mitochondria from A; (D) image analysis of C processed by the *black top hat* filter. EB and R123 double staining experiment: (E) EB fluorescence image of peripheral mitochondria; (F) R123 fluorescence image of central mitochondria and (G) merged image with peripheral mitochondria in red and central mitochondria in green.

3.2. *Mitochondria in multidrug resistant MCF-7/DX carcinoma cells*

In the MCF-7/DX cells the pattern of EB (Fig. 2A) and R123 fluorescence (Fig. 2B) was very different from that observed in the parental sensitive cells, since both probes stained only peripheral mitochondria but not central ones. As shown in Fig. 2I, the merged image (in yellow) is due to the overlapping of the EB fluorescence image (in red) with that of R123 (in green) (Fig. 2G and Fig. 2H). The intense R123 and EB fluorescence of peripheral mitochondria indicated, respectively, that these mitochondria have a high membrane potential and display a strong binding to EB (Fig. 2A and B). Since EB colocalizes with R123 that is a well established marker of mitochondria, this experiment further confirms that EB is a probe of mitochondria in living cells. The morphology and organization of these peripheral mitochondria were better resolved by image analysis of the data obtained from single staining experiments (Fig. 2C–F). In this cell line, the same pattern of punctate organelles, organized in rosette like clusters, was obtained for peripheral mitochondria.

Unexpectedly, the treatment of MCF-7/DX cells with verapamil – a well-known revertant of multidrug resistance and a calcium channel blocker[24,25] – allowed us to detect a pool of mitochondria in the central cytoplasm region, as reported and discussed in our previous R123 study[22]. Indeed, in the presence of this revertant, the pattern of EB and R123 fluorescence was changed (Fig. 3): peripheral mitochondria kept their high EB fluorescence (Fig. 3A) but loosed their R123 fluorescence (Fig. 3B), while a population of central mitochondria with elongated morphology acquired a strong R123 and a weak – but appreciable – EB fluorescence (Fig. 3B and A). Under these conditions, a strong EB staining of the nucleolar area (Fig. 3A) became evident. The merged image from the double staining experiment with EB (Fig. 3C) and R123 (Fig. 3D) shows peripheral mitochondria and nucleoli in red

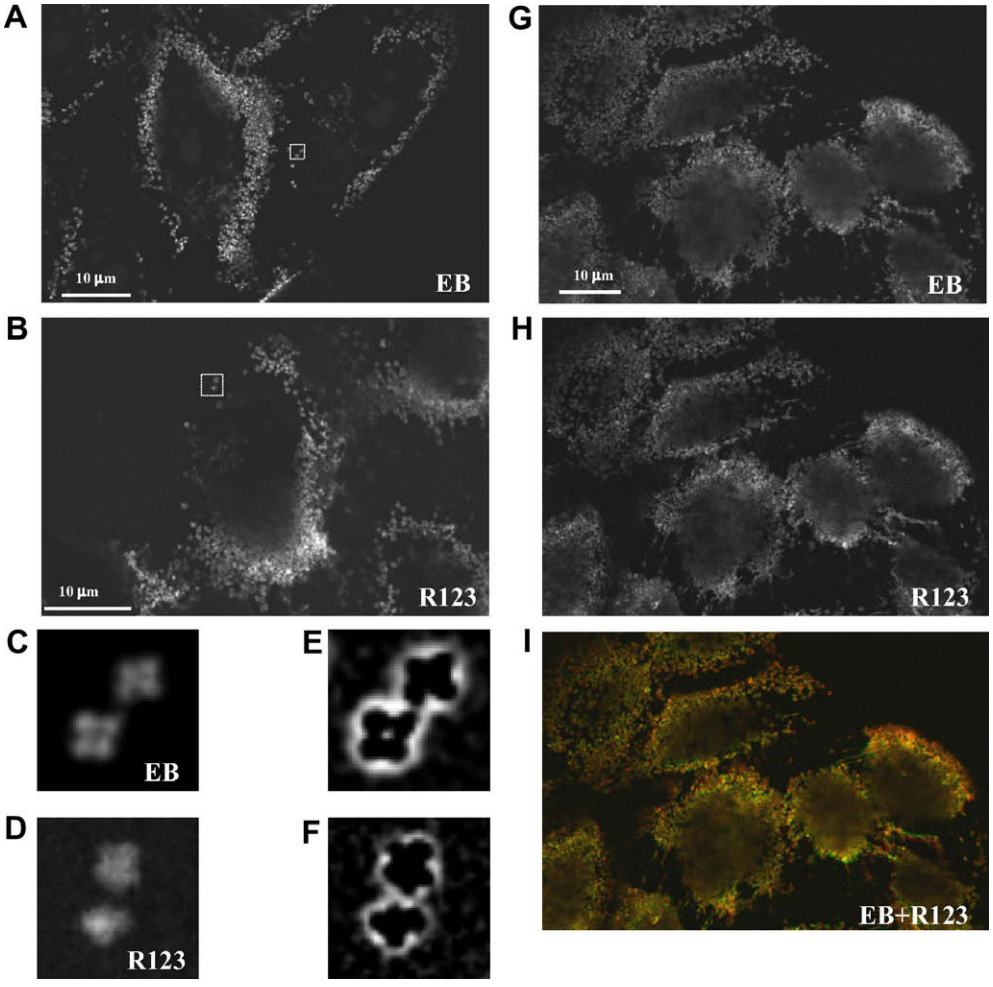

Fig. 2 – Fluorescence images of mitochondria in multidrug-resistant human breast MCF-7/DX carcinoma cells. Fluorescence images of mitochondria in (A) after EB and in (B) after R123 staining. Only peripheral mitochondria are observed in both cases. (C) enlarged image of mitochondria from A; (D) enlarged image of mitochondria from B. (E) image analysis of C and (F) image analysis of D, after *black top hat* filter. EB and R123 double staining experiment: (G) EB fluorescence image; (H) R123 fluorescence image and (I) merged image showing the colocalisation of the two probes on peripheral mitochondria.

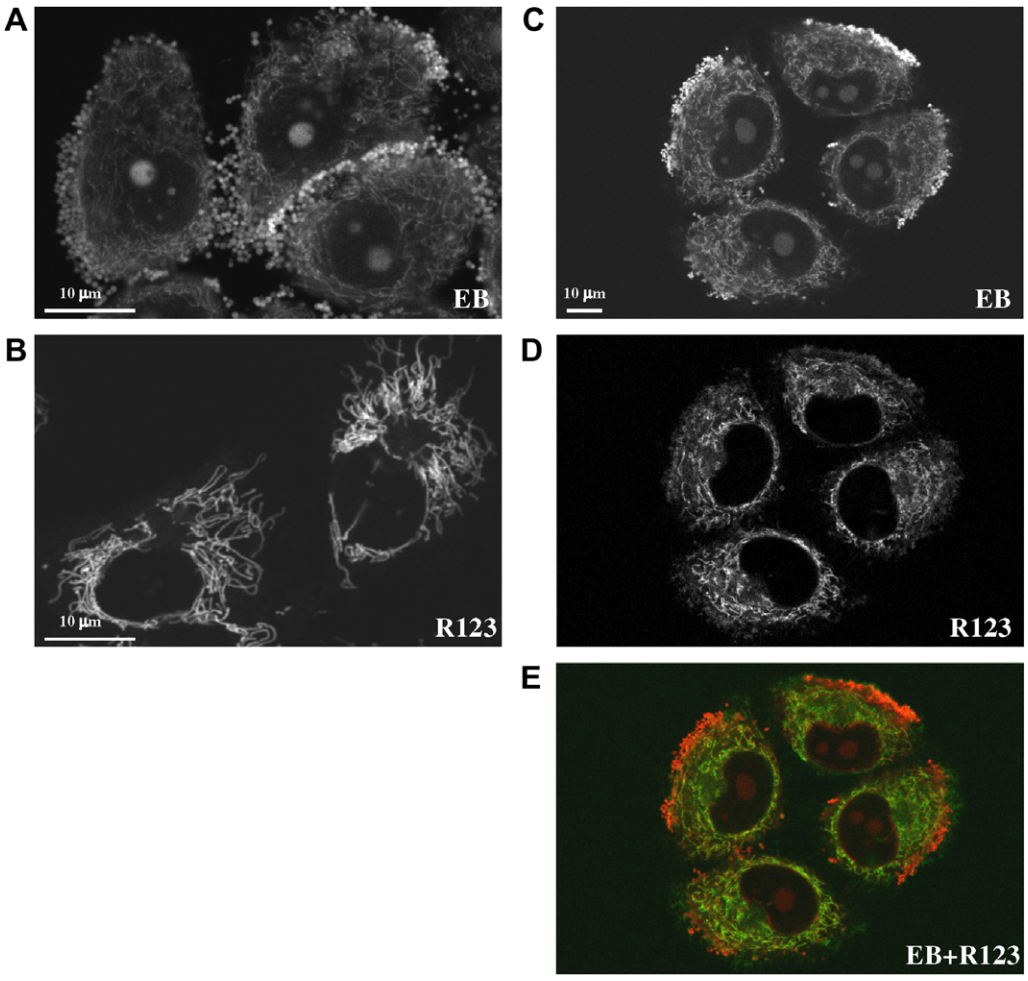

Fig. 3 – Fluorescence images of mitochondria in MCF-7/DX carcinoma cells treated with verapamil. Mitochondria stained in the presence of verapamil by EB in (A) and by R123 in (B).The two images indicate that the fluorescence pattern of sensitive cells is restored in the presence of the MDR revertant. EB and R123 double staining experiment: (C) EB fluorescence of peripheral mitochondria, (D) R123 fluorescence of central mitochondria and (E) merged image with peripheral mitochondria in red and central mitochondria in green, displaying the spatial localisation of the two mitochondria populations as in sensitive MCF-7 cells.

(EB) and central mitochondria in green (R123) (Fig. 3E), a fluorescence pattern similar to that seen in sensitive MCF-7 cells (Fig. 1G).

These results, therefore, confirm the presence of two pools of mitochondria with different energetic state, localization and morphology in multidrug resistant MCF-7/DX cells. In addition, it also indicates that verapamil is able to change the membrane potential of the two populations and to restore the functional state of mitochondria observed in sensitive MCF-7 cells. Interestingly, in the same MCF-7/DX cell line verapamil restored the high Ca^{2+} uptake of sensitive cells, as reported by De Bernardi and Brooker.[24]

These results demonstrate that two distinct populations of mitochondria, are present both in MCF-7 and in MCF-7/DX carcinoma cells, with different membrane potential, cellular localization, morphology and different EB fluorescence pattern.

3.3. *Mitochondria in immortalized MCF-10A cells*

In order to investigate if two populations of mitochondria also existed in the immortalised epithelial MCF-10A cell line, a good model system for non-malignant epithelial cells, we studied the intracellular distribution of EB and R123 by a double staining experiment (Fig. 4A–C). As shown in Fig. 4A and B, only one population of mitochondria was present in these non-tumour cells. No punctate mitochondria with high EB fluorescence and rosette-like organisation were seen at the cell periphery, opposite to what was found for carcinoma cells. It is interesting to note that in MCF-10A cells EB fluorescence was not homogenously distributed within central mitochondria, where highly fluorescent spots were observed. These round spots, with a diameter of about 0.8 μm, can be identified as mitochondria nucleoids, which are assemblies of mtDNA and associated proteins, already found in

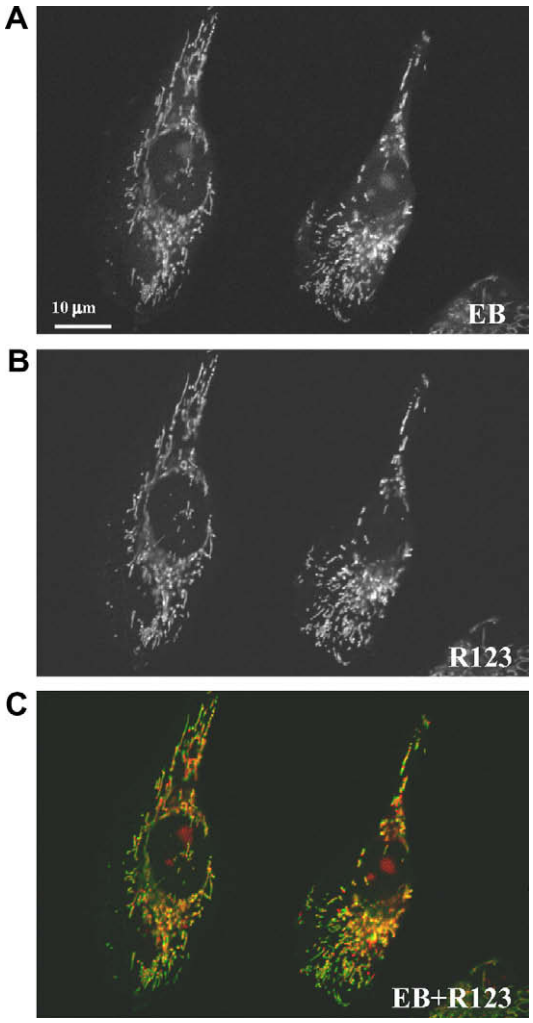

Fig. 4 – Mitochondria in MCF-10A cells. EB and R123 double staining experiment: (A) fluorescence image of mitochondria after EB staining and (B) after R123 staining. (C) Merged image with EB stained mitochondria in red and R123 stained mitochondria in green. Only the population of central mitochondria is observed in these non-malignant cells. While R123 fluorescence is evenly distributed along each organelle, well-defined spots can be recognised after EB staining within central mitochondria (A).

mitochondria of several cell lines.[20,26] In addition, in this cell line nucleoli were also stained by EB, as can be seen in the merged image of Fig. 4C.

3.4. *Mitochondria in A549 carcinoma cells*

We also examined the intracellular distribution of EB in the human lung carcinoma A549 cells (Fig. 5 and Fig. 6), which are known to overexpress the lung resistant protein LRP. Two mitochondria populations were detected by the EB staining experiment presented in Fig. 5A, where both central and peripheral mitochondria display a high EB fluorescence. Using R123, the presence of two pools of mitochondria was confirmed, displaying a different R123 fluorescence intensity and, therefore, a different membrane potential (Fig. 5D). These two populations corresponded to those observed in the breast carcinoma cells: elongated mitochondria in the bulk cytoplasm and punctate mitochondria at the cell periphery. Interestingly, the morphology of the latter mitochondria is very similar to that reported in Fig. 1C and D and Fig. 2C–F, therefore indicating that the peculiar morphology and spatial organization of peripheral mitochondria were common features of all the examined carcinoma cells.

Furthermore, EB fluorescent spots of about 0.8 μm in size can be clearly seen within central mitochondria, as in the case of MCF-10A cells (Fig. 4A). Again these spots, which display a fluorescence intensity varying one from the other (Figs. 5A and 6A and B), can be identified as mitochondria nucleoids.[20,26] A rather uniform fluorescence (Fig. 5D) was instead observed in these mitochondria after R123 staining. Therefore, in the merged image of the double staining experiment (Fig. 6A and B), EB fluorescent nucleoids (red) were clearly visible over the R123 fluorescence (green) evenly distributed in the organelles. In addition, also nucleoli were strongly fluorescent after EB staining (Figs. 5A and 6A).

In Fig 6C, we report the EB and R123 merged image to better highlight the localization of peripheral mitochondria in A549 cells. This image clearly shows that peripheral mitochondria, stained by EB and R123, are also distributed along thin filaments that are seen to protrude from the plasma membrane toward neighboring cells. This pattern of filaments decorated by punctate mitochondria was also seen in multidrug resistant MCF-7/DX cells (Fig. 2G–I) Interestingly, it has been recently discovered a new cell-to-cell communication consisting of thin membranous tubular structures, containing F-actin filaments as major cytoskeleton component.[27] The function of these tunneling nanotubes (TNT) is to allow intercellular signaling and transport of cellular components, including mitochondria.[27]

As conclusive remark, we note that the different fluorescence patterns of the two probes, observed in A549 cells as well as in MCF-7 cells, reflected the different interaction of EB and R123, respectively, with mtDNA and with the mitochondria membrane potential. These results indicate that complementary mitochondria probes should be used to fully characterize the complete mitochondria system of living cells.

4. Discussion

Using EB as a mtDNA probe and R123 as a potentiometric marker, we studied mitochondria in carcinoma cells under living condition by LSCFM with photon counting detection. In all the examined carcinoma cell lines, we detected two distinct mitochondria populations characterized by a different intracellular localization, morphology and membrane potential: a population of elongated mitochondria in the bulk cytoplasm and a population of punctate mitochondria organized in rosette-like assemblies at the cell periphery. In addition, the two mitochondria populations were characterized by a different EB fluorescence, with peripheral mitochondria displaying a strong intensity.

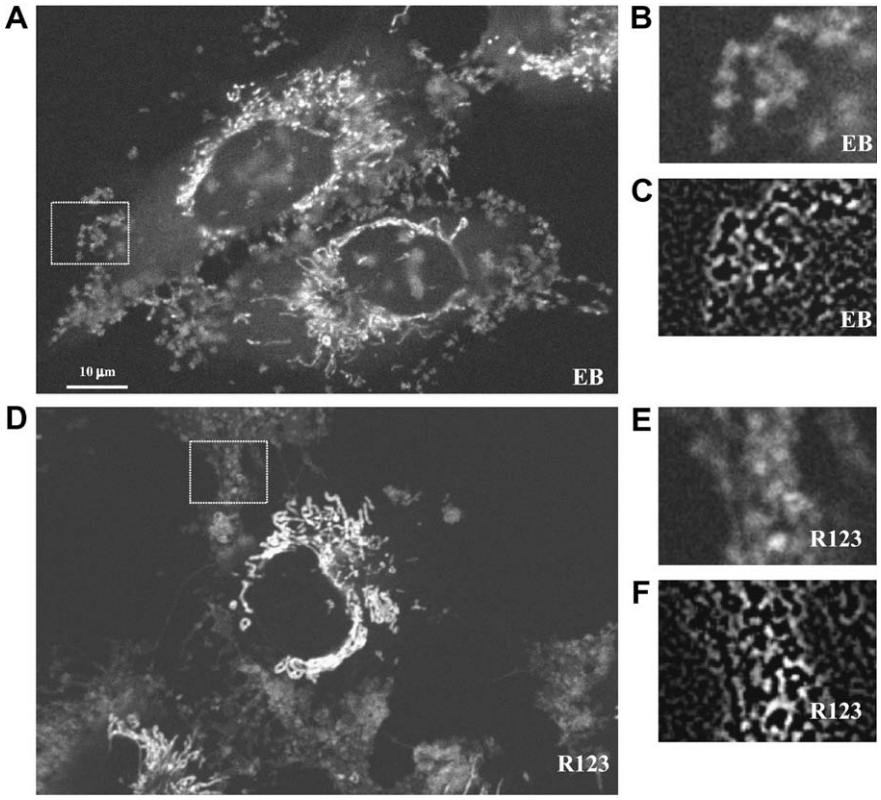

Fig. 5 – Mitochondria in A549 carcinoma cells. Central and peripheral mitochondria stained by EB in (A); enlarged image of peripheral mitochondria from A in (B) and its image analysis in (C) after *black top hat* filter. Central and peripheral mitochondria stained by R123 in (D); enlarged image of peripheral mitochondria from D in (E) and its image analysis in (F) after *black top hat* filter. Image analysis shows an identical morphology for peripheral mitochondria stained by the two probes.

Interestingly, the presence of the peripheral mitochondria population with high EB fluorescence was found to be a peculiar feature of carcinoma cells, since in immortalized epithelial MCF-10A cells – a good experimental system of non-malignant human breast epithelial cells[28] – only a single mitochondria population with elongated morphology was detected in the bulk cytoplasm.

Concerning these findings, it should be noted that while it is well known that the intensity of R123 fluorescence is related to the mitochondria membrane potential, the very different EB fluorescence intensity observed for the two mitochondria populations in breast carcinoma cells was an unexpected result, since EB was considered an overall marker of mitochondria in living cells due to its binding to mtDNA.[12,16] Our results, instead, indicated that while peripheral mitochondria were highly fluorescent in all the examined carcinoma cells after EB staining, central mitochondria displayed only a very weak fluorescence. Actually, we should recall that EB, when intercalated in double[29] and triple[30] DNA helices, displays a much higher fluorescence yield than when free in aqueous solution. Therefore, the strong fluorescence intensity of EB in mitochondria could be taken as evidence of its intercalation in mtDNA, while the absence of EB fluorescence might result from a lack of mtDNA accessibility. Similar differences in EB accessibility have been recently reported for nuclear DNA in living proliferating S2 monkey kidney cells,[18] where, by fluorescence lifetime and anisotropy decay measurements, only a few regions of nuclear DNA were found to be accessible to EB intercalation. The authors of this study suggested that the accessible sites could correspond to internucleosomal regions, where DNA is free from histones and proteins, as well as to regions of DNA in active replication and/or transcription. Indeed, in carcinoma cells, we observed a high EB fluorescence in nucleoli (Figs. 1A, 3A and E, 4C, 5A and 6A), where histone-free DNA can be found in active transcription.

Concerning mtDNA, it is important to recall that a strong interaction of EB with replicating mtDNA in living cells has been reported in literature over the years. In particular, EB was found to inhibit the synthesis of mtDNA in living cells by affecting DNA polymerase γ or by deleting RNA primers necessary to initiate the mtDNA replication.[31–33] Also the transcription and translation of mtDNA genes were inhibited in the presence of EB.[33,34] Furthermore, a long term EB treatment was widely used to obtain ρ° cells, human cell lines lacking mtDNA.[35]

All these studies suggest that, similarly to what happens in nuclear DNA[18], EB in mitochondria may interact by intercalation only with actively replicating and transcribing mtDNA. If this would be the case, the strong EB fluorescence from peripheral mitochondria of MCF-7 and MCF-7/DX cells might indicate the interaction of EB with mtDNA molecules which

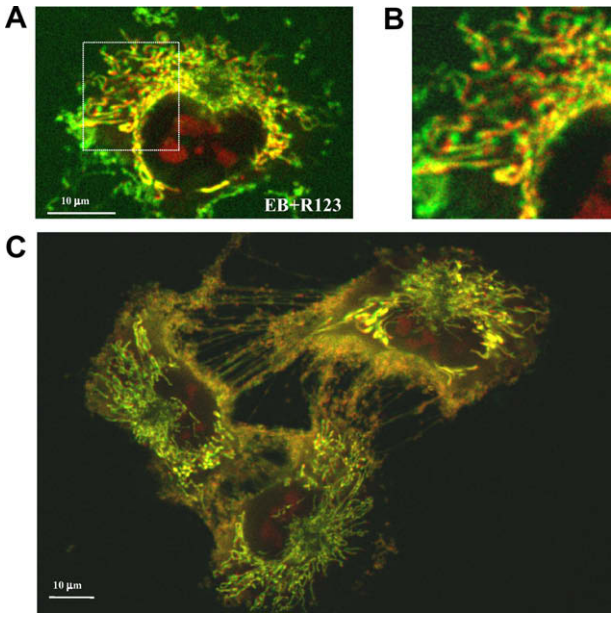

Fig. 6 – EB and R123 double staining images of mitochondria in A549 carcinoma cells. (A) Merged image double staining experiment and (B) high magnification image of central mitochondria from (A). EB and R123 display a different fluorescence pattern: highly EB fluorescent nucleoids (red) are seen within each organelle, while the fluorescence of R123 (green) is homogenously distributed along the entire mitochondrion. In (C), a double staining image of A549 cells, displaying the two pools of mitochondria highlights the intracellular distribution of peripheral mitochondria also along filaments protruding from the membrane and bridging neighbouring cells.

are in active transcription and/or replication. On the contrary, the absence of EB fluorescence in central mitochondria would suggest that their mtDNA – not accessible to EB – is not in active replication or transcription. Interestingly, a weak EB fluorescence in central mitochondria was observed in MCF-7/DX cells after the treatment with verapamil, suggesting that this MDR revertant, which restores the membrane potential of central mitochondria as in sensitive cells, also affects the activation of mtDNA for replication and transcription.

Similarly, in A549 cells the different EB fluorescence intensity of nucleoids in central mitochondria may be related to a different number of actively replicating and/or transcribing mtDNA molecules, in agreement with the findings that in each nucleoid mtDNA replicates independently, and that nucleoids can be also synthetically or transcriptionally inactive.[21,26,36]

Similarly, a non-uniform fluorescence intensity of nucleoids has been reported for mitochondria in mouse living cells stained by ditercalinium chloride[37], an intercalating dye which shares several properties with EB. Interestingly, these authors suggested that highly fluorescent nucleoids could contain a higher number of mtDNA molecules in active replication and/or transcription.

The presence of active mtDNA only in peripheral mitochondria of the breast carcinoma cells examined here seems, therefore, to indicate that an enhanced biogenesis and/or an enhanced transcription is at work in this mitochondria population. Considering that peripheral mitochondria have been observed only in carcinoma cells, but not in immortalized epithelial MCF-A cells, their enhanced mtDNA activity might be related to the tumorigenic potential of carcinoma cells.[38]

In addition, it is interesting to note that, as recently reported in literature,[39–42] the morphology and intracellular localization of mitochondria is related to their functions and bioenergetic activity in the cell. The different membrane potential and morphology of central and peripheral mitochondria in sensitive and in multidrug resistant MCF-7DX carcinoma cells can be, therefore, taken as an indication of a different bioenergetic status of the two cell lines. Indeed, an increased energy requirement is expected for MCF-7/DX carcinoma cells, since in presence of MDR these cells were found to be characterized by a higher motility, invasivity and metastatic capacity than their parental sensitive MCF-7 cells.[43–45] Interestingly, as shown in Fig. 2B, the presence of peripheral mitochondria with active membrane potential is correlated with the fibroblast-like morphology that carcinoma cells acquire in the presence of multidrug resistance and at the onset of the metastatic progression.[22,46] In addition, we should note that in resistant cells peripheral mitochondria have been also observed along protruding filaments joining neighbouring cells, as shown in Figs. 2I and 6C. It has been recently suggested that these structures formed when connected cells start to migrate.[27] Furthermore, the presence of multiple pools of mitochondria in a single cell has been recently found to play a fundamental role in shaping intracellular Ca^{2+} signaling.[47,48] Since an active membrane potential is required for mitochondrial calcium uptake, our results can also suggest that sensitive and multidrug resistant MCF-7 cells might differ in their calcium homeostasis and signalling.[49] The high membrane potential of peripheral mitochondria in multidrug resistant cells could then indicate, similarly to what observed for pancreatic acinar cells,[39] that this pool of mitochondria, close to the plasma membrane, might be involved in the Ca^{2+} uptake and buffering required for the different energetic metabolism of these transformed cells.

In this study we therefore report the presence of two distinct populations of mitochondria in human breast and lung carcinoma cell lines, characterized by a different EB fluorescence, membrane potential, cellular localization and morphology. An important variation in the fluorescence intensity of EB in the two mitochondria populations might reflect a different EB accessibility to mtDNA, which in turn could be related to its transcription and replication status.

These results, first of all, indicate that EB cannot be taken as an overall marker of mtDNA, and that complementary mitochondria probes should be used to characterize the whole system of mitochondria in living cells. Additionally, as shown here by EB and R123 staining, the detection of different mitochondria populations at single cell level in carcinoma cells could offer a powerful tool for understanding the role of mitochondria in the tumour transformation. Indeed, the presence of peripheral mitochondria, which has been found to be

a peculiar feature only of transformed cells, could be required by the different energetic needs of the tumour phenotype.

To better understand the EB fluorescence response of mitochondria, further LSCFM and molecular biology experiments are now in progress on other cell lines where the mtDNA activity can be modulated by external effectors. In this way, it might be possible to examine if the level of EB fluorescence intensity can be used – as a complementary tool – to monitor the mtDNA transcription and replication in living cells.

Conflict of interest statement

None declared.

Acknowledgements

We are grateful to Carla Smeraldi for kindly revising the language. S.M.D. acknowledges the financial support of the grant F.A.R. (Fondo di Ateneo per la Ricerca) of the University of Milano-Bicocca.

REFERENCES

1. Kroemer G, Reed JC. Mitochondrial control of cell death. *Nat Med* 2000;**6**:513–9.
2. Schapira AHV. Mitochondrial disease. *Lancet* 2006;**368**:70–82.
3. Gogvadze V, Orrenius S, Zhivotovsky B. Mitochondria in cancer cells: what is so special about them? *Trends Cell Biol* 2008;**18**:165–73.
4. Ortega AD, Sánchez-Aragó M, Giner-Sánchez D, et al. Glucose avidity of carcinomas. *Cancer Lett* 2009;**276**:125–35.
5. Kroemer G, Pouyssegur J. Tumor cell metabolism: cancer's Achilles' heel. *Cancer Cell* 2008;**13**:472–82.
6. Carew JS, Huang P. Mitochondrial defects in cancer. *Mol. Cancer* 2002;**1**:9.
7. Xie CH, Naito A, Mizumachi T, et al. Mitochondrial regulation of cancer associated nuclear DNA methylation. *Biochem Biophys Res Commun* 2007;**364**:656–61.
8. Feinberg AP, Ohlsson R, Henikoff S. The epigenetic progenitor origin of human cancer. *Nat Rev Genet* 2006;**7**:21–33.
9. Nikolaev AI, Martynenco AV, Kalmyrzaev BB, et al. Increased expression of several mitochondrial genes in human and monkey B-cell non-Hodgkin lymphomas. *Mol Biol* 2001;**35**:108–14.
10. Grandemange S, Seyer P, Carazo A, et al. Stimulation of mitochondrial activity by p43 overexpression induces human dermal fibroblast transformation. *Cancer Res* 2005;**65**:4282–91.
11. Rizzuto R, Brini M, Pizzo P, Murgia M, Pozzan T. Chimeric green fluorescent protein as a tool for visualizing subcellular organelles in living cells. *Curr Biol* 1995;**5**:635–42.
12. Coppey-Moisan M, Brunet AC, Morais R, Coppey J. Dynamical change of mitochondrial DNA induced in the living cell by perturbing the electrochemical gradient. *Biophys J* 1996;**71**:2319–28.
13. Kuznetsov AV, Usson Y, Leverve X, Margreiter R. Subcellular heterogeneity of mitochondrial function and dysfunction: evidence obtained by confocal imaging. *Mol Cell Biochem* 2004;**256**(/257):359–65.
14. Sikder S, Reyes JM, Moon CS, et al. Noninvasive mitochondrial imaging in live cell culture. *Photochem Photobiol* 2005;**81**:1569–71.
15. Ramey NA, Park CY, Gehlbach PL, Chuck RS. Imaging mitochondria in living corneal endothelial cells using autofluorescence microscopy. *Photochem Photobiol* 2007;**83**:1325–9.
16. Hayashi J-I, Takemitsu M, Goto Y, Nonaka I. Human mitochondria and mitochondrial genome function as a single dynamic cellular unit. *J Cell Biol* 1994;**125**:43–50.
17. Favard C, Pager J, Locker D, Vigny P. Incorporation of ethidium bromide in the Drosophila salivary gland approached by microspectrofluorometry: evidence for the presence of both free and bound dye in the nuclei of cells in viable conditions. *Eur Biophys J* 1997;**25**:225–37.
18. Tramier M, Kemnitz K, Durieux C, et al. Restrained torsional dynamics of nuclear DNA in living proliferative mammalian cells. *Biophys J* 2000;**78**:2614–27.
19. Durieux C, Brunet AC, Geeraert V, Coppey J, Coppey-Moisan M. A transient decrease of electrochemical gradient stabilizes DNA structural change in single mitochondria of living cells. *Biol Cell* 1999;**91**:597–604.
20. Spelbrink JN, Li FY, Tiranti V, et al. Human mitochondrial DNA deletions associated with mutations in the gene encoding Twinkle, a phage T7 gene 4-like protein localized in mitochondria. *Nat Genet* 2001;**28**:223–31.
21. Iborra FJ, Kimura H, Cook PR. The functional organization of mitochondrial genomes in human cells. *BMC Biol* 2004;**2**: 9–23.
22. Villa AM, Doglia SM. Mitochondria in tumor cell studied by laser scanning confocal microscopy. *J Biomed Opt* 2004;**9**:385–94.
23. Davis S, Weiss MJ, Wong JR, Lampidis TJ, Chen LB. Mitochondrial and plasma membrane potentials cause unusual accumulation and retention of rhodamine 123 by human breast adenocarcinoma-derived MCF-7 cells. *J Biol Chem* 1985;**260**:13844–50.
24. DeBernardi MA, Brooker G. High-content kinetic calcium imaging in drug-sensitive and drug-resistant human breast cancer cells. *Meth Enzymol* 2006;**414**:317–35.
25. Tsuruo T, Iida H, Nojiri M, Tsukagoshi S, Sakurai Y. Circumvention of vincristine and Adriamycin resistance in vitro and in vivo by calcium influx blockers. *Cancer Res* 1983;**43**:2905–10.
26. Garrido N, Griparic L, Jokitalo E, Wartiovaara J, van der Bliek AM, Spelbrink JN. Composition and dynamics of human mitochondrial nucleoids. *Mol Biol Cell* 2003;**14**:1583–96.
27. Gurke S, Barroso JFV, Gerdes H-H. The art of cellular communication: tunneling nanotubes bridge the divide. *Histochem Cell Biol* 2008;**129**:539–50.
28. Spink BC, Cole RW, Katz BH, et al. Inhibition of MCF-7 breast cancer cell proliferation by MCF-10A breast epithelial cells in coculture. *Cell Biol Int* 2006;**30**:227–38.
29. LePecq JB, Paoletti C. A fluorescent complex between ethidium bromide and nucleic acids, physical–chemical characterization. *J Mol Biol* 1967;**27**:87–106.
30. Mergny JL, Collier D, Rougee M, Montenay-Garestier T, Helene C. Intercalation of ethidium bromide into a triple-stranded oligonucleotide. *Nucleic Acids Res* 1991;**19**:1521–6.
31. Leibowitz RD. The effect of ethidium bromide on mitochondrial DNA synthesis and mitochondrial DNA structure in HeLa cells. *J Cell Biol* 1971;**51**:116–22.
32. Tarrago-Litvak L, Viratelle O, Darriet D, et al. The inhibition of mitochondrial DNA polymerase gamma from animal cells by intercalating drugs. *Nucleic Acids Res* 1978;**5**:2197–210.
33. Hayakawa T, Noda M, Yasuda K, et al. Ethidium bromide-induced inhibition of mitochondrial gene transcription suppresses glucose-stimulated insulin release in the mouse

pancreatic beta-cell line betaHC9. *J Biol Chem* 1998;**273**:20300–7.
34. Galper JB. Mitochondrial protein synthesis in HeLa cells. *J Cell Biol* 1974;**60**:755–63.
35. King MP, Attardi G. Human cells lacking mtDNA: repopulation with exogenous mitochondria by complementation. *Science* 1989;**246**:500–3.
36. Legros F, Malka F, Frachon P, Lombes A, Rojo M. Organization and dynamics of human mitochondrial DNA. *J Cell Sci* 2004;**117**:2653–62.
37. Okamaoto M, Ohsato T, Nakada K, et al. Ditercalinium chloride, a pro-anticancer drug, intimately associates with mammalian mitochondrial DNA and inhibits its replication. *Curr Genet* 2003;**43**:364–70.
38. Starcevic SL, Elferink C, Novak RF. Progressive resistance to apoptosis in a cell lineage model of human proliferative breast disease. *J Natl Cancer Inst* 2001;**93**:776–82.
39. Park MK, Ashby MC, Erdemli G, Petersen OH, Tepikin AV. Perinuclear, perigranular and sub-plasmalemmal mitochondria have distinct functions in the regulation of cellular calcium transport. *EMBO J* 2001;**20**:1863–74.
40. Bahamonde MI, Valverde MA. Voltage-dependent anion channel localises to the plasma membrane and peripheral but not perinuclear mitochondria. *Eur J Physiol* 2003;**446**:309–13.
41. Skulachev VP, Bakeeva LE, Chernyak BV, et al. Thread-grain transition of mitochondrial reticulum as a step of mitoptosis and apoptosis. *Mol Cell Biochem* 2004;**256–257**:341–58.
42. Kuznetsov AV, Troppmair J, Sucher R, et al. Mitochondrial subpopulations and heterogeneity revealed by confocal imaging: possible physiological role? *Biochim Biophys Acta* 2006;**1757**:686–91.
43. Beckner ME, Stracke ML, Liotta LA, Schiffmann E. Glycolysis as primary energy source in tumor cell chemotaxis. *J Natl Cancer Inst* 1990;**82**:1836–40.
44. Weinstein RS, Jakate SM, Dominguez JM, et al. Relationship of the expression of the multidrug resistance gene product (P-glycoprotein) in human colon carcinoma to local tumor aggressiveness and lymph node metastasis. *Cancer Res* 1991;**51**:2720–6.
45. Ristow M. Oxidative metabolism in cancer growth. *Curr Opin Clin Nutr Metab Care* 2006;**9**:339–45.
46. Amuthan G, Biswas G, Ananadatheerthavarada HK, et al. Mitochondrial stress-induced calcium signaling, phenotypic changes and invasive behavior in human lung carcinoma A549 cells. *Oncogene* 2002;**21**:7839–49.
47. Parekh AB. Mitochondrial regulation of intracellular Ca^{2+} signaling: more than just simple Ca^{2+} buffers. *News Physiol Sci* 2003;**18**:252–6.
48. Varadi A, Cirulli V, Rutter GA. Mitochondrial localization as a determinant of capacitative Ca^{2+} entry in HeLa cells. *Cell Calcium* 2004;**36**:499–508.
49. Parekh AB. Ca^{2+} microdomains near plasma membrane Ca^{2+} channels: impact on cell function. *J Physiol* 2008;**586**: 3043–54.